



# ASTENA, a new mission concept for an Advanced Surveyor of Transient Events and Nuclear Astrophysics

F. Frontera<sup>1,2</sup>, E. Virgili<sup>1</sup>, V. Carassiti<sup>3</sup>, C. Guidorzi<sup>1</sup>, P. Rosati<sup>1</sup>, L. Amati<sup>2</sup>,  
N. Auricchio<sup>2</sup>, L. Bassani<sup>2</sup>, R. Campana<sup>2</sup>, E. Caroli<sup>2</sup>, F. Fuschino<sup>2</sup>, R. Gilli<sup>2</sup>,  
C. Labanti<sup>2</sup>, A. Malizia<sup>2</sup>, M. Orlandini<sup>2</sup>, J. B. Stephen<sup>2</sup>, G. Stratta<sup>2</sup>, S. Del Sordo<sup>3</sup>,  
G. Ghirlanda<sup>4</sup>, S. Brandt<sup>6</sup>, C. Budtz-Joergensen<sup>6</sup>, I. Kuvvetli<sup>6</sup>, R. M. Curado da Silva<sup>7</sup>,  
J. M. Maia<sup>7,9</sup>, M. Moita<sup>7</sup>, and P. Laurent<sup>8</sup>

<sup>1</sup> Università di Ferrara – Dept Fisica e Scienze della Terra, Via Saragat 1, I-44122 Ferrara, Italy, e-mail: [frontera@fe.infn.it](mailto:frontera@fe.infn.it)

<sup>2</sup> Istituto Nazionale di Astrofisica (INAF) – Osservatorio di Astrofisica e Scienza dello Spazio, Via Gobetti 101, I-40129 Bologna, Italy

<sup>3</sup> INFN, Section of Ferrara, Via Saragat 1, I-44122 Ferrara, Italy

<sup>4</sup> INAF-IASF Palermo, Via Ugo la Malfa, 153, 90146 Palermo PA, Italy

<sup>5</sup> INAF-OAB Merate, Via E. Bianchi, 46, 23807 San Rocco LC, Italy

<sup>6</sup> DTU–Space, Elektrovej, DK-2800 Kgs. Lyngby, Copenhagen, Denmark

<sup>7</sup> University of Coimbra–LIP, Rua Larga, 3004-516 Coimbra, Portugal

<sup>8</sup> CEA–Irfu, Saclay, Orme des merisiers, 91191 Gif sur Yvette, France

<sup>9</sup> Physics Department, University of Beira-Interior, 6200 Covilha, Portugal

**Abstract.** Within the context of the European project AHEAD, the study of a new concept of high energy mission named ASTENA (Advanced Surveyor of Transient Events and Nuclear Astrophysics) has been started. The mission includes a set of broad band (2 keV–20 MeV) Wide Field Monitors with imaging, spectroscopy and polarimetric capabilities (WFM-IS), and a large effective area broad-band (50–600 keV) Narrow Field Telescope (NFT) with focusing capabilities based on the use of an advanced Laue lens with unprecedented imaging, spectroscopy and polarimetric sensitivity. ASTENA is expected to be a real breakthrough in the gamma-ray energy band, opening a new window in high energy astrophysics. A short description of the mission concept is reported.

**Key words.** soft gamma-ray astronomy – instrumentation – GRBs – nuclear astrophysics

## 1. Introduction

Within the context of the European project AHEAD (integrated Activities in the High Energy Astrophysics Domain), a Work

Package (WP 9) was devoted to gamma-ray astronomy.

The goal was establishing the most relevant science goals for future gamma-ray missions and thus propose possible solutions for

achieving these goals. The conclusion of an established Science Advisory Group (SAG) was that Gamma-Ray Bursts (GRBs) and Nuclear Astrophysics were the top-priority themes for a gamma-ray mission. Three proposals of mission concepts were selected by an Instrument Working Group (IWG) and thus admitted for an evaluation study through simulations. One of the three was an *Advanced Surveyor of Transient Events and Nuclear Astrophysics* (ASTENA, PI P. Rosati).

We present here a short summary of the ASTENA mission concept and its main goals. An extended paper on this subject is in preparation.

## 2. ASTENA configuration

A sketch of the ASTENA configuration we assumed for the proposal submitted to the IWG is shown in Fig. 1.

It consists of a Wide Field Monitor-Imaging Spectrometer (WFM-IS) working in the passband 2 keV–20 MeV and a Narrow Field Telescope (NFT) in the passband 50–600 keV. The NFT is based on a Laue lens with a 3 m diameter and 20 m focal length. Through a 15 m deployable boom, a Position Sensitive Detector (PSD) is located in the lens focus. The WFM-IS is deployed in flight. In this way the satellite can be accommodated in the fairing of a Soyuz launcher, but, with a different design, also in the fairing of a Vega C launcher.

### 2.1. WFM-IS main features

The WFM-IS consists of 6 blocks of 3 detection units, accommodated as shown in Fig. 1, with two of them offset in one direction by  $\pm 20^\circ$ . Instead of blocks of 3 detection units, blocks of two units are being investigated for improving its imaging capability.

Each WFM-IS unit is conceptually similar to the XGIS units aboard the THESEUS mission (Amati et al. 2018). It consists of an array of detection elements, each made of a scintillator bar (CsI(Tl) or similar) 5 cm long with an hexagonal cross section of about 75 mm<sup>2</sup>, viewed by two Silicon Drift Detectors (SDD)

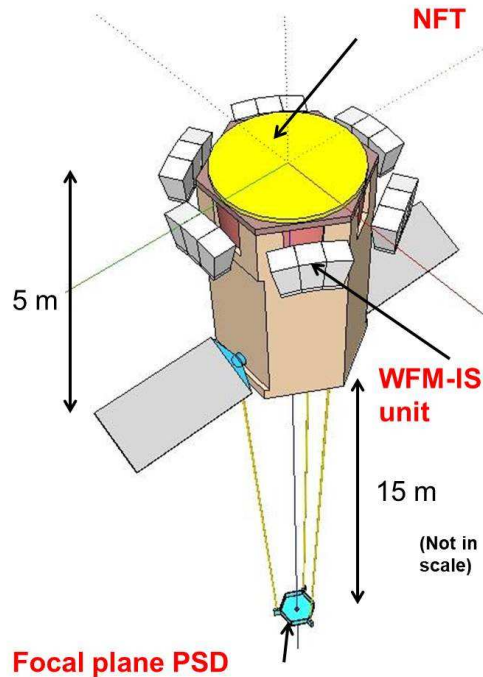


**Fig. 1.** Possible configuration of the ASTENA mission concept in flight. Blocks of two WFM-IS detectors instead of three are being considered for improving its imaging capabilities.

0.45 mm thick, one on the top (side of entrance of the celestial photons) and other on the bottom. The energy losses in the SDD or in the scintillator are recognized thanks to their different rise time of the produced pulses, as shown in Fig. 2. The top SDD allows for a spatial resolution of about 1 mm for the low energy photons that lose their energy in the SDD, and a position sensitivity of about 5 mm for the high energy photons that lose their energy in the scintillator bar. Each detection unit is passively shielded on its sides and is surmounted by a field collimator and a coded mask, in order to get imaging with a point source location accuracy of 1 arcmin up to 30 keV and 5 arcmin up to 150 keV. The instrument field of view is about 1 sr up to 150 keV, and about  $2\pi$  beyond. The total expected effective area of the WFM-IS through the mask is about 4000 cm<sup>2</sup> up to 30 keV, 6000 cm<sup>2</sup> up to 150 keV and about

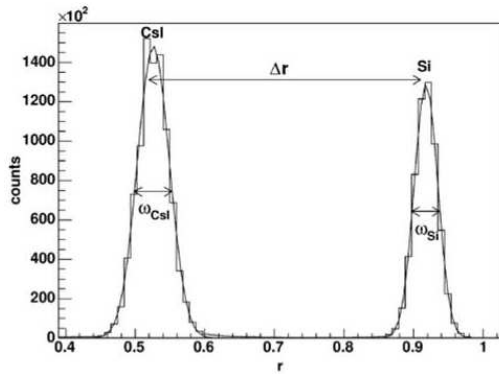


**Fig. 2.** Pulse shape distribution of the WFM-IS detection elements. Reprinted from Marisaldi et al. (2004).

1.2 m<sup>2</sup> beyond 200 keV. Thanks to the hexagonal shape of the scintillator bars, the WFM-IS is particularly suitable to be used also as a Compton polarimeter. Above 200 keV, exploiting the Compton kinematics, it is also possible to get crude information about the incident direction of the high energy photons.

Given the WFM-IS high effective area, it is possible to achieve higher sensitivities than the current and planned instrumentation for transient events. In photons/(cm<sup>2</sup> s), the expected  $3\sigma$  sensitivity in a 10 s integration time ranges from about 40 mCrab in 2–10 keV to about 100 mCrab in 30–150 keV, and to 800 mCrab in 0.15–1 MeV.

Thanks to these performances, the WFM-IS is particularly suitable to be triggered by celestial transient events, like short and long (also low luminosity) GRBs, X-/gamma-ray counterparts of Gravitational Wave events, Tidal Disruption Events, etc, deriving for each of them their celestial location with 1 arcmin accuracy for prompt follow up with the NFT, derive their prompt emission spectrum and the polarization status at high energies (>80 keV).

## 2.2. NFT main features

The NFT focusing optics is based on a spherical Laue lens (see, e.g., the review by Frontera & von Ballmoos 2010) that reflects hard X-/soft gamma-rays for diffraction from crys-

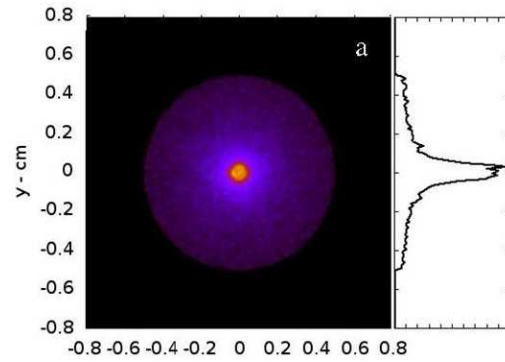


**Fig. 3.** Expected on-axis NFT PSF, for small crystal misalignments and curvature radius distortion (see text).

tals in Laue configuration. The diffracting crystals are bent tiles of Si and Ge with reflecting planes (111), cross section of  $30 \times 10$  cm<sup>2</sup> and curvature radius of 40 m. The consequent focal length of the lens is 20 m. Due to the curvature, the inner structure of the reflecting planes is quasi-mosaic (Sumbaev 1957; Ivanov et al. 2005) with a secondary curvature of the reflecting planes. The crystals are disposed on rings with the outermost ring radius of 1.5 m. With this size, the projected geometric area is about 7 m<sup>2</sup>. The expected performances of a lens made of bent crystals of only Ge(111) with the same focal length is discussed elsewhere, taking also in the account crystal tile misalignments and radial distortion of the crystal curvature (see Virgilli et al. (2017) and Virgilli et al. in these proceedings). For the lens development status see Virgilli et al. in these proceedings. In the case of small crystal misalignments (< 10 arcsec) and  $\leq 5\%$  radial distortion of the crystal curvature, with both conditions already almost achieved in lab (see Virgilli et al. in these proceedings), the expected on-axis Point Spread Function (PSF) (Virgilli et al. 2017) is that shown in Fig. 3. Through Monte Carlo simulations it has also been possible to derive the off-axis PSF (Virgilli et al. 2017), and to estimate the Field of View of the lens (about 4 arcmin) and its angular resolution (30 arcsec).

Concerning the NFT focal plane detector, starting from the lens optical properties, its

requirements (3-D position sensitivity, detection efficiency, etc) are given elsewhere (Khalil et al. 2015). The adopted configuration consists of 4 layers of drift strip detectors of CdZnTe(CZT) (Kuvvetli et al. 2014), each layer with a cross section a  $80 \times 80 \text{ mm}^2$  and a thickness of 20 mm. A development activity is in progress. The goal is to achieve a 3-D position sensitivity of  $300 \mu\text{m}$  and a detection efficiency higher than 80% in the entire operational energy range of the NFT. With these position sensitivity properties, the focal plane detector has been demonstrated to be also sensitive to photon polarization for Compton interactions (Caroli et al. 2018).

The expected NFT Minimum Detectable Polarization (MDP), at 99% confidence level in the total range 50–600 keV, ranges from  $\sim 2\%$  for a 100 mCrab source in  $10^5 \text{ s}$  to  $\sim 30\%$  for a 1 mCrab source in the same observation time. As realistic value a detector modulation factor of 0.6 for a 100% polarized beam is assumed (Caroli et al. 2018).

The NFT sensitivity for an on-axis source with energy  $E$  has also been estimated (Fig. 4) after deriving the effective area of the lens at different energies  $E$  in energy intervals  $\Delta E = E/2$ , the detection efficiency of the focal plane detector and using the background level discussed elsewhere (Virgilli et al. 2017). Notice that in the lenses the effective area depends on the energy bandwidth, because increasing the bandwidth we increase the number of crystal tiles that reflect photons in that bandwidth. We use  $\Delta E = E/2$  to compare the sensitivity of the NFT with that of other instruments/missions.

Also the sensitivity to narrow lines has been estimated by simulations, following the procedure discussed elsewhere (Virgilli et al. 2017). In the case of small crystal tile misalignments and small distortions of the crystal curvature radius as discussed above, for observation times of  $10^5 \text{ s}$ , at  $3\sigma$  confidence level, the sensitivities to lines range from  $3.7 \times 10^{-7} \text{ photons}/(\text{cm}^2 \text{ s})$  at 100 keV to  $2.3 \times 10^{-5} \text{ photons}/(\text{cm}^2 \text{ s})$  at 500 keV.

With these performances and sensitivities, the NFT is expected to perform an unprecedented leap forward in the study of the hard X-/soft gamma-ray sky, as it is discussed else-

where (Frontera et al., in preparation). We limit here to list some of the most significant achievements expected with NFT:

- First deep study of the high energy spectra of GRB afterglows;
- Determination of the polarization level of the GRB high energy afterglow;
- Determination of the origin of the 511 keV positron annihilation line from the Galactic Centre region, a 40 yr mystery of high energy astrophysics. It could be due to point-like sources, like microquasars or, among other possibilities, to conversion of dark matter–anti-dark matter into electron–positron pairs with the production of the 511 keV positron annihilation line.
- Detection and mapping with 30 arcsec resolution of the nuclear lines from supernovae (SNe), either those emitted at early times in supernova explosions like the 158 keV line due to the  $^{56}\text{Ni}$  decay, either those still found in supernova remnants, like the 67.9 and 78.4 keV  $^{44}\text{Ti}$  lines from Cas A.
- Hard X-/soft gamma-ray spectral properties of AGNs (e.g., high energy cutoff of radio quiet AGNs, Blazar hard X-/soft gamma-ray spectrum still unknown).

### 3. Conclusions

ASTENA is the first mission concept based on a broad band hard X-/soft gamma-ray optics (50–600 keV). It explores with unprecedented sensitivity the high energy transient sky (prompt and afterglow emission of short and long GRBs, low luminosity GRBs, X-/gamma-ray counterparts of Gravitational Wave Events, Tidal Disruption events, etc) and their properties (spectrum, light curves, polarization level).

For the first time, in the soft gamma-ray band, it provides:

- a point source localization accuracy below 1 arcmin;
- an angular resolution of about 30 arcsec;
- a continuum spectrum sensitivity orders of magnitude better than the current instrumentation

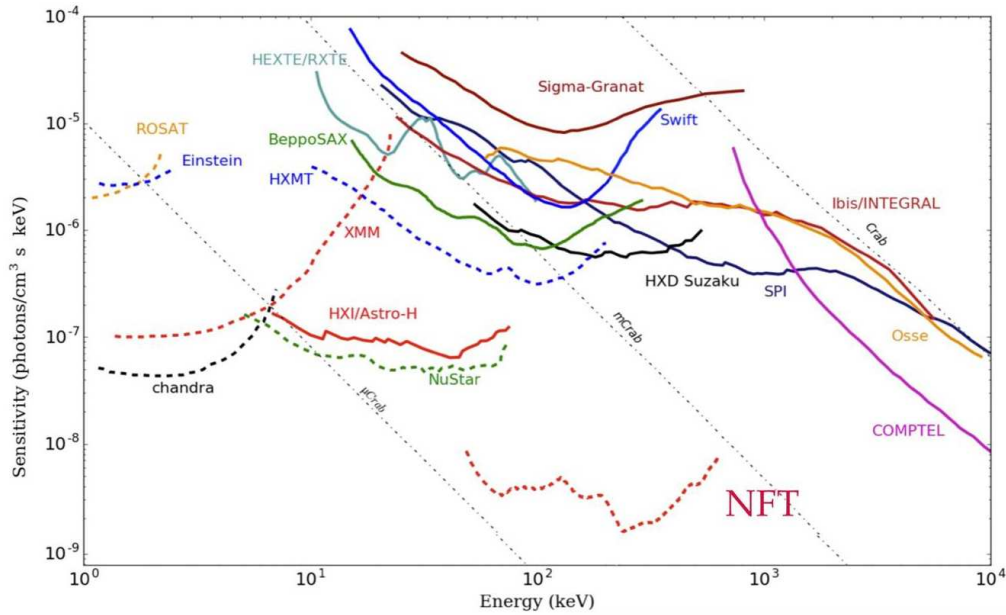


**Fig. 4.** NFT  $3\sigma$  continuum sensitivity with energy  $E$  from 50 to 600 keV in  $10^5$  s observation time and bandwidth  $\Delta E = E/2$ . See text for further information.

Thanks to its angular resolution and high sensitivity to lines, the origin of the positron annihilation line from the GC region (a mystery 50 yrs old) can be unveiled and the mapping of nuclear lines in supernova explosions and remnants investigated.

*Acknowledgements.* We acknowledge the support by AHEAD (integrated Activities in the High Energy Astrophysics Domain), a project approved within the EU Framework Programme for Research and Innovation Horizon 2020.

## References

- Amati, L., O'Brien, P., Götz, D., et al. 2018, *Advances in Space Research*, 62, 191
- Caroli, E., Moita, M., da Silva, R., et al. 2018, *Galaxies*, 6, 69
- Frontera, F. & von Ballmoos, P. 2010, *X-Ray Optics and Instrumentation*, 2010, 215375
- Ivanov, Y. M., Petrunin, A. A., & Skorobogatov, V. V. 2005, *Journal of Experimental and Theoretical Physics Letters*, 81, 99
- Khalil, M., et al. 2015, *Nuclear Instruments and Methods in Physics Research A*, 786, 59
- Kuvvetli, I., Budtz-Jørgensen, C., Zappettini, A., et al. 2014, *Proc. SPIE*, 9154, 91540X
- Marisaldi, M., Labanti, C., & Soltau, H. 2004, *IEEE Transactions on Nuclear Science*, 51, 1916
- Sumbaev, O. I. 1957, *Soviet Physics JETP*, 5, 1042
- Virgilli, E., Valsan, V., Frontera, F., et al. 2017, *Journal of Astronomical Telescopes, Instruments, and Systems*, 3, 044001